Available online at www.sciencedirect.com

SciVerse ScienceDirect

Acta Materialia 60 (2012) 339–348

Acta MATERIALIA

www.elsevier.com/locate/actamat

Energetics of (1 1 4) twinning in B2 NiTi under coupled shear and shuffle

Tawhid Ezaz [a], Huseyin Sehitoglu [a,*], Hans Jürgen Maier [b]

[a] Department of Mechanical Science and Engineering, University of Illinois at Urbana-Champaign, 1206 W. Green St., Urbana, IL 61801, USA
[b] University of Paderborn, Lehrstuhl für Werkstoffkunde, D-33095 Paderborn, Germany

Received 21 July 2011; received in revised form 21 September 2011; accepted 21 September 2011
Available online 4 November 2011

Abstract

The (1 1 4) twin growth in the austenitic regime in NiTi (B2 lattice) is characterized precisely at the atomistic scale. This twinning mode is consistent with experimental observations but has not been well understood despite its importance. Combined shears, shuffles and interface shifts operate in a complex way to generate the (1 1 4) twin. Pure shear on the (1 1 4) plane results in a "pseudo-twin", and interchange shuffles are necessary to convert this to a "reflective" twin and render a lower energy state. Additional atomic shifts at the twin–matrix interfaces result in "sharp" boundaries, further lowering the energy barriers. We established the energy barrier to be 148 mJ m^{-2} during (1 1 4)[2 2 $\bar{1}$] twin boundary growth of four layers at a time. The entire potential energy surface and the mean energy path during twinning can be derived from our simulations, providing the required insight into the atomistic processes involved.

Keyword: Deformation twinning; B2 NiTi; ab initio; (1 1 4) shuffle

1. Introduction

1.1. Deformation twinning in NiTi B2 phase

Fundamental discoveries concerning the underlying mechanisms responsible for the unusual behavior of novel materials have opened up new opportunities in materials science and engineering. The exceptional physical and mechanical properties of NiTi are widely known [1]. Under thermoelastic transformation, NiTi reverts from the austenitic (B2) phase to the monoclinic (B19′) phase. Above the A_f temperature, stress-induced martensite formation occurs up to the M_d temperature. Above M_d, this transformation can no longer be stress-induced. Plastic deformation above M_d is of considerable interest to shape memory research. Plastic deformation can be manifested via slip or twinning, depending on the crystal orientations. Under ausforming, which refers to shaping in the austenitic regime, NiTi alloys are deformed at temperatures above the M_d temperature where they exhibit considerable plasticity and ductility (exceeding 25%). This high ductility is unusual because the B2 intermetallic alloys are expected to exhibit limited ductility [2]. In the B2 phase of NiTi, slip occurs in $\{0\,1\,1\}\langle 1\,0\,0\rangle$, which permits glide only in three systems. Given that at least five independent active systems are needed to accommodate arbitrary deformations, the ductility in this simple cubic intermetallic compound is attributed to the presence of additional twin systems. B2 NiTi undergoes mechanical twinning during processing operations or during the B2 to B19′ transformation [3].

Previous work on twinning in NiTi B2 phase has attracted considerable attention. Sinclair and co-workers at Stanford University have made important contributions, and Refs. [4–7] provide extensive discussion of the (1 1 4) twinning. Chumlyakov and colleagues [8,9] in Russia have also reported observation of (1 1 4) twins, and Nishida and colleagues [10,11] in Japan provided further evidence of this. All these research groups have focused on experiments and confirmation of the (1 1 4) twin system via transmission electron microscopy (TEM) investigations. While the

* Corresponding author. Tel.: +1 217 333 4112; fax: +1 217 244 6534.
E-mail address: huseyin@illinois.edu (H. Sehitoglu).

1359-6454/$36.00 © 2011 Acta Materialia Inc. Published by Elsevier Ltd. All rights reserved.
doi:10.1016/j.actamat.2011.09.032

experimental studies provide the end state (of twinned domains), we provide here the insight into the energy barriers necessary for a better comprehension of the evolution of displacements and boundary shifts.

In the austenitic phase of NiTi, twinning is frequently observed in the $(1\,1\,4)[2\,2\,\bar{1}]$ system, generating mirror symmetry along the boundary. These observations are made with ex situ electron diffraction pattern matching; however, it is a challenge to determine experimentally the precise motion of atoms during twinning. Twins are developed over femtoseconds and growth of layers occurs on the nanometer scale with complex paths precluding precise in situ interrogation. Furthermore, $(1\,1\,4)[2\,2\,\bar{1}]$ is not a regular glide plane for B2 NiTi and no twinning partial is observed experimentally in this system. In the absence of an intrinsic fault as a precursor, the twinning partials are not viewed under ex situ conditions. For example, in face-centered cubic (fcc) alloys, the intrinsic faults are readily observed because they are in a metastable position (position "s" in the graph in Table 1). The absence of twinning partials represents a basic difference in the twinning process in B2 NiTi from that of a face-centered cubic (fcc) or body-centered cubic (bcc) metal. In this paper, we focus on the details of atomic arrangements of twin growth in the $(1\,1\,4)[2\,2\,\bar{1}]$ system in B2 NiTi, which has been elusive, and provide a complete energetic description of the process.

1.2. Classification of twin formation and growth

The deformation twin formation and growth mechanism can be classified into two major cases as shown in Table 1. We propose that such a classification facilitates the understanding of twinning. In case 1, for example, in cubic crystal structures, twin formation and growth is mediated by a step-by-step glide of the twinning partial. It is known that a full dislocation splits into partials, since energetically the split dislocations can overcome a lower barrier while breaking away as partial dislocations. As shown in Table 1 (case 1), in fcc metals, a full $a/2[1\,0\,\bar{1}]$ dislocation splits into two partial dislocations, the $a/6[1\,1\,\bar{2}]$ leading and $a/6[2\,\bar{1}\,\bar{1}]$ trailing partial, which glide in the same $(1\,1\,1)$ plane. In the case of bcc metals, splitting to three twin partials occurs. In fcc, the energy barriers for the two partials are shown with blue points as the generalized stacking fault energy (GSFE) curve. GSFE provides a comprehensive description of this energy barrier, and describes its possible slip direction. During twin formation, only leading twinning partials nucleate at consecutive planes and generate ledges. This grows the twin perpendicular to the direction of the partial dislocation glide. The mechanism is illustrated in the schematic in Table 1 as case 1.

Barriers for twin formation are usually quantified with the generalized planar fault energy (GPFE, shown with a red line), which quantifies the energy landscape for twin nucleation on consecutive planes. The point "u" denotes the unstable stacking fault energy. Since a stacking fault is the first step of twin formation in fcc metals, the GSFE and GPFE share a common energy path up to layer 1 (point "s" in case 1). Detailed descriptions of the GSFE and the GPFE can be found elsewhere [12].

However, the twin formation mechanism in ordered metals with lattices of lower symmetry is distinct from that found in fcc and bcc metals since shearing will not create a mirror structure along the boundary. Also, deformation twins can occur in planes and directions (e.g. $(1\,1\,4)[2\,2\,\bar{1}]$) that differ from slip. In this case (case 2), the structures are considered to be built up of atoms grouped around the Bravais lattice points and these groups of atoms shear as rigid bodies. Additional shuffles must occur to obtain a mirror reflection [13]. Shuffles are local rearrangements of atoms that permit reflective symmetry. In this case, the slip and twin evolution are again described with GSFE and GPFE curves (with shuffle). As shown with the blue dotted line, slip in these systems will induce a high-energy barrier. The barrier is significantly lowered once atoms are locally exchanged by additional shuffle (red line). Shear and shuffle are not sequential, and in this paper we point out to their exact coupling.

Returning to the B2 NiTi literature, deformation twin planes are known to be $(1\,1\,2)$ and $(1\,1\,4)$, and pseudotwinning has also been suggested [5–7,9,11]. Pseudotwinning, originally proposed by Cahn [14], results in an orthorhombic structure, hence the use of the prefix "pseudo". Krishnan and Maji [15] pointed out that, upon close scrutiny of the diffraction patterns of a reported pseudotwin, in B2 NiTi the TEM results correspond to the $(1\,1\,4)$ type twin. More recently Nishida et al. [11] identified $(1\,1\,4)$ and $(1\,1\,2)$ twin planes as the most important ones, and at the same time showed the formation of other twin types as well; a strong resemblance to a "self-accommodating" morphology was noted. Recently, energy barrier and atomic arrangement calculations have been reported for the $(1\,1\,2)$ type of twin [16]. However, the exact mechanism for $(1\,1\,4)$ twin formation and its energy barrier have yet to be established; this is the focus of this paper. The $(1\,1\,4)$ twinning is a significant twinning mechanism in B2 NiTi that, as we will show, can occur at lower stresses as compared to the $(1\,1\,2)$ case. Because of its complexity, we first provide a detailed background of $(1\,1\,4)$ twinning.

1.3. Combined shear and shuffle in $(1\,1\,4)$ twin formation

Twins in $(1\,1\,4)$ planes are classified as $\Sigma 9$ boundaries based on coincident site lattice (CSL) notation. The CSL value is calculated by taking the ratio of the total number of atoms at the interface to those atoms that are in coincidental sites from each lattice. However, the atomic movement in the $(1\,1\,4)$ twin formation is complicated because of the local arrangements of the atoms. Goo et al. [7] considered both shear and shuffle for $(1\,1\,4)$ twin formation. According to his hypothesis, the $(1\,1\,4)$ twinning mode involves shearing of atoms with a magnitude of $s = 1/\sqrt{2}$ in the $[2\,2\,\bar{1}]$ direction, followed by half the atoms of the

Table 1
Classification of twin formation mechanisms in cubic or ordered intermetallics. The displacement in the energy barrier curves is usually expressed as a function of the lattice constant.

Material	Twin system	Energy barrier	Schematic of twin formation
Case 1	*Twinning partials form (No Shuffle)*		
FCC (Au, Ag, Cu, Ni etc.) [12]	FCC, $(1\,1\,1)[1\,1\,\bar{2}]$ $\frac{a}{2}[1\,0\,\bar{1}] \rightarrow \frac{a}{6}[1\,1\,\bar{2}] + \frac{a}{6}[2\,\bar{1}\,\bar{1}]$	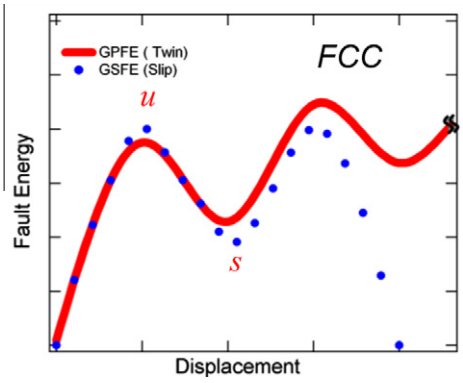	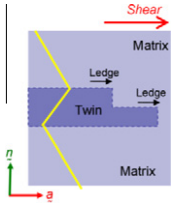
BCC (Fe, Mo, Ta, Va etc.) [13–15]	BCC, $(1\,1\,\bar{2})[1\,1\,1]$ $\frac{a}{2}[1\,1\,1] \rightarrow \frac{a}{6}[1\,1\,1] + \frac{a}{6}[1\,1\,1] + \frac{a}{6}[1\,1\,1]$		
B19′ NiTi [16]	B19′, (001)[100] $a[1\,0\,0] \rightarrow \frac{a}{2}[1\,0\,0] + \frac{a}{2}[1\,0\,0]$		
Case 2	*Twinning partials do not form*		
NiTi B19′ [16]	(100)[001]⟨011⟩ Type II(20−1)[−10−2]	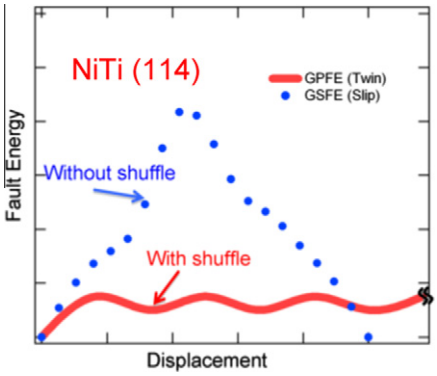	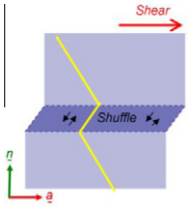
NiTi B2	$(1\,1\,4)[2\,2\,\bar{1}]$ (this study) (100)[001]		

(1 1 0) plane shuffling $a/2$ in the [0 0 1] direction (all shuffling atoms displace in the same direction). Moberly [4] proposed an alternative mechanism in which atoms shear in the opposite $[\bar{2}\,\bar{2}\,1]$ direction, followed by a shuffling in the [1 1 1] and $[\bar{1}\,\bar{1}\,\bar{1}]$ directions. However, Moberly's proposed mechanism requires a shear of $\sqrt{2}$, a high shear magnitude, which has been suggested for other systems [17,18]. In addition, both Goo et al.'s and Moberly's type of model requires net displacement of atoms away from the interface, giving effectively rows of vacancies on the twin side of the interface—and hence requiring an increase in the volume. This is not apparent from TEM observations and violates the view of twinning as a non-dilatational deformation mechanism. Further discussions on this will be provided later.

For ordered alloys, Christian and Laughlin [19] proposed a shuffling mechanism where atoms rearrange locally after every four layers of shear, and hence lower the global energy of the system. This mechanism is also discussed in the review by Mahajan and Christian [20]. In the (1 1 4) twinning case, four layers of atoms are sheared simultaneously since the interplanar distance in the (1 1 4) plane is rather low ($0.226a$). We analyze shearing of four layers of atoms simultaneously with a coupled shuffle of atoms of (1 1 0) planes in the [0 0 1] direction oblique to the shear direction. In this paper, we elaborate how this coupled shear and shuffle mechanism for the (1 1 4) twin formation can occur and determine the twinning barrier magnitude.

A schematic of this twin growth from four layers to eight layers is shown in Fig. 1. From an existing four-layer

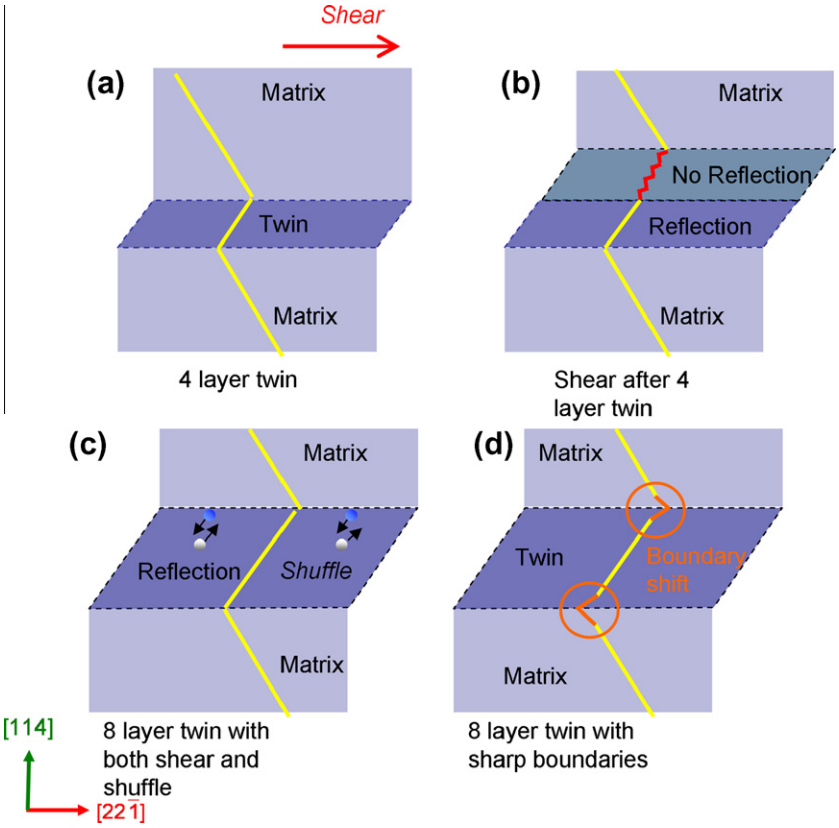

Fig. 1. Schematic of the (1 1 4) twin growth mechanism for an existing four-layer twin (a). (b) A shearing magnitude of $1/\sqrt{2}$ moves half the atoms in the preferred location; however, a mirror reflection is not generated along the twin boundary. (c) Shuffles in the desired direction create mirror symmetry along the twin boundary. (d) Boundary shift at the upper and lower interfaces decreases the barrier further.

Table 2
Shear and shuffle parameters for twin growth in the $(1\,1\,4)[2\,2\,\bar{1}]$ system. Shear ε and shuffle η magnitudes are normalized by the maximum shear displacement $2a/9[2\,2\,\bar{1}]$ and the shuffle displacement a/2, respectively.

Twin shear system	Shear magnitude	Shuffle plane	Shuffle magnitude	Transition state	Boundary shift
$(1\,1\,4)[2\,2\,\bar{1}]$	$1/\sqrt{2}$	(1 1 0)	$a/2\langle 0\,0\,1\rangle$	Normalized shear, $\varepsilon = 0.82$[a] Normalized shuffle, $\eta = 0.22$[b]	$a/18[2\,2\,\bar{1}]$and $a/18[\bar{2}\,\bar{2}\,1]$

[a] Normalized with respect to the shear displacement $2a/9[2\,2\,\bar{1}]$.
[b] Normalization with respect to $a/2$.

twin (shown in Fig. 1a), a shear magnitude of $1/\sqrt{2}$ moves half the atoms to their preferred position for the twin. However, this shear generates a pseudo-structure as shown in Fig. 1b with the shaded blue region. A pseudo-twin is energetically unstable and undergoes local rearrangement of atoms via a shuffle mechanism. Shuffling of atoms with shear completes the growth mechanism and extends the twin to an eight-layer structure (shown in Fig. 1c). The twin structure, however, is not stable at the interface and the interaction of atomic rows parallel to the (1 1 4) plane lead to an additional horizontal shift of the upper and the lower boundary (shown in Fig. 1d). This configuration is called the "sharp boundary". Here, we note that a twin with a sharp boundary retains mirror symmetry along the compositional plane; only the atoms at the boundary shift to lower the interfacial energy configuration. For the $(1\,1\,4)[2\,2\,\bar{1}]$ twinning system, this shift is found to be $a/18[2\,2\,\bar{1}]$ and $a/18[\bar{2}\,\bar{2}\,1]$ for the upper and lower boundaries, respectively. The shear and shuffle parameters for the $(1\,1\,4)[2\,2\,\bar{1}]$ system are noted in Table 2. Precise calculations are needed to illustrate the exact coupling of shear and shuffle during twin growth. In the present paper, we determine this coupling.

The shuffle direction coupled with a $1/\sqrt{2}$ magnitude shear is a point of discussion since three alternatives are possible [19,20]. According to the first alternative, proposed by Goo et al. [7], Ni and Ti atoms shuffle unidirectionally in [0 0 1] to reach the final stable configuration (shown in Fig. 2a). However, unidirectional shuffle does not satisfy local equilibrium and induces a moment field during the shuffle. Also, as noted earlier, the mechanism requires a void and interstitial at the interfaces that cause

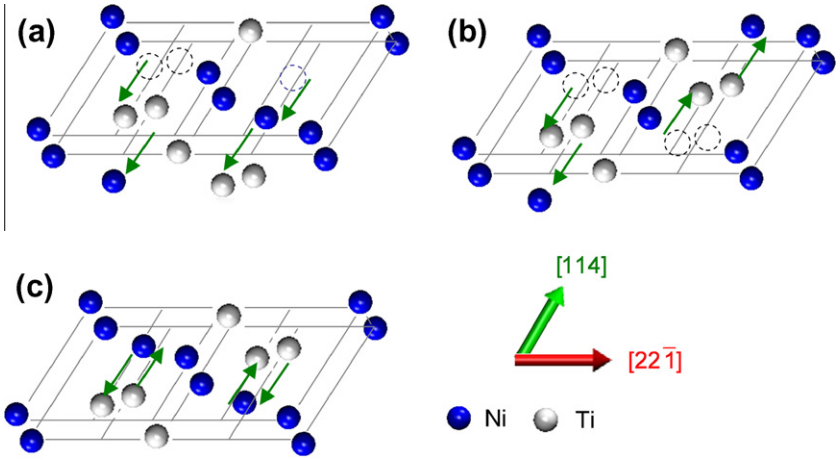

Fig. 2. Schematic of alternative shuffle modes in {1 1 4} twinning of B2 NiTi. (a) Unidirectional shuffle of Ni and Ti in the [0 0 1] direction during twin growth in one direction. (b) Long-range bidirectional shuffle between the Ni and Ti atoms maintaining the equilibrium moment between the atoms. (c) Short range bi-directional local shuffle of atoms maintaining the equilibrium. (After Christian and Laughlin [19,20].)

an increase in volume. We calculated the energy barrier for Goo's case as 1210 mJ m^{-2}, a very high value, which precludes its occurrence. Christian and Laughlin [19] proposed two mechanisms with bidirectional shuffle that avoid the generation of this moment field. The first bidirectional shuffle is long range (Fig. 2b), which, nevertheless, requires inclusion of a void and interstitials at the twin interface similar to Goo et al.'s case and increases the twin volume. The second bidirectional shuffle is short range and requires a local interchange between the Ni and Ti atoms followed by shear (Fig. 2c). Since this mechanism does not require any increase in twin volume, we investigate the energetics of this shuffling mechanism coupled with shear.

The atomic arrangement of the proposed growth mechanism is illustrated in Fig. 3. Here, we note that only a partial simulation box is shown depicting the twinned structure. As noted above, a shear of magnitude $1/\sqrt{2}$ moves half of the atoms to a preferred position and generates a pseudo-structure. This pseudo-structure has in-plane Ti–Ti or Ni–Ni bonding instead of out-of-plane Ni–Ti bonding in the [0 0 1] direction. This is shown with the black curly parenthesis and the red dotted line in Fig. 3b. Similar atoms in close proximity require high bonding energy, which induces the shuffle between Ni and Ti atoms. A shuffle reduces the global energy of the system and generates a B2 structure within the twin. In addition, a mirror

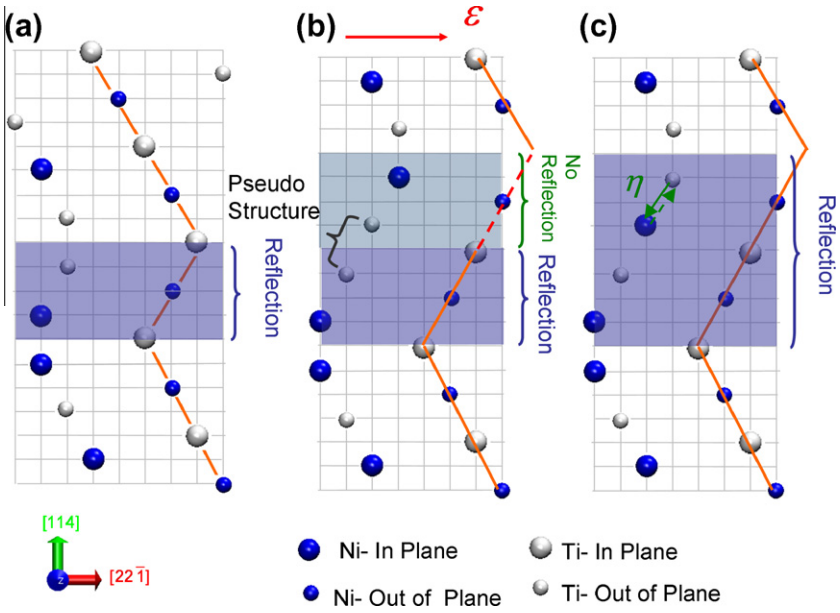

Fig. 3. (a) Atomic projection of a four-layer twin in NiTi B2 from the [1 1̄ 0] direction. (b) A shear ε of magnitude $1/\sqrt{2}$ creates a pseudo-twin structure. (c) Internal arrangement between Ni and Ti atoms in the [0 0 1] and [0 0 1̄] directions in successive rows of the shuffle plane extend the twin to eight layers.

reflection is generated along the (1 1 4) plane, hence extending the twin to eight layers.

As noted earlier, in the (1 1 4)[2 2 $\bar{1}$] system, a complete sequence of shear and shuffle generates a twin of four layers. An energetic measurement during this coupled shear shuffle sequence will provide the necessary insight into the atomistic processes controlling the twinning and will serve as the foundation for a better understanding of the process, which is the objective of this paper.

2. Methods

First-principles calculations were utilized to establish the GSFE, potential-energy surface (PES), the minimum energy path (MEP) and the transition state (TS) associated with twin growth; these parameters are defined later in the paper. The energy cost of a possible dislocation motion in the (1 1 4)[2 2 $\bar{1}$] system was investigated in terms of the GSFE. For the (1 1 4)[2 2 $\bar{1}$] system, the fault energy was measured by shearing one elastic half space of a (1 1 4) plane relative to another in the [2 2 $\bar{1}$] shear direction. During calculation of the GSFE, a complete landscape of fault energy was investigated, which requires a displacement of an interplanar distance in the respective shear direction. Therefore, the total displacement magnitude in the [2 2 $\bar{1}$] directions was calculated to be $a|[2\ 2\ \bar{1}]| = 3a$. The GSFE for the (1 1 4)[2 2 $\bar{1}$] system is plotted against the displacement in each layer, u_x, which is normalized by its required displacement, $a|[2\ 2\ \bar{1}]|$.

The structural energy cost, $\Delta E(\eta, \varepsilon)$, for twin growth with coupled shear and shuffle, during the (1 1 4) twin growth process can be represented by a planar energy surface. Here, E, ε, η represents the potential energy field, normalized by both shear and shuffle. The shear parameter, ε, is normalized by the shear displacement $2a/9[2\ 2\ \bar{1}]$ and the shuffle, η, by the average nearest-neighbor distance, a/2. We note that $\Delta E(\eta, \varepsilon)$ refers to the energy differential between the fourth layer and the eighth layer twin structure. We calculated the energetics of twin growth from four to eight layers, and the results ruled out the possibility of mechanical coupling of the twin boundary. A mechanical coupling arises from the interaction energy of upper and lower twin boundaries, necessitating consideration of fourth and higher layers to characterize twin growth behavior [21].

In most bcc structures, a perfect reflective twin boundary is not energetically stable and upon relaxation a sharp boundary is observed as a translational state [22–24]. Sharp boundaries at the upper and lower interfaces lower the energy configuration, which results in a local displacement of atoms of magnitude $a/18[2\ 2\ \bar{1}]$ and $a/18[\bar{2}\ \bar{2}\ 1]$, respectively (shown in Fig. 4). For clarity of the elaboration of the shear and shuffle mechanism, in Fig. 3, we show the reflective boundaries prior to relaxation. We used spin-polarized, ab initio calculation to properly determine the undeformed and deformed energy states of NiTi austenite during the {1 1 4} twin growth. The ab initio calculations

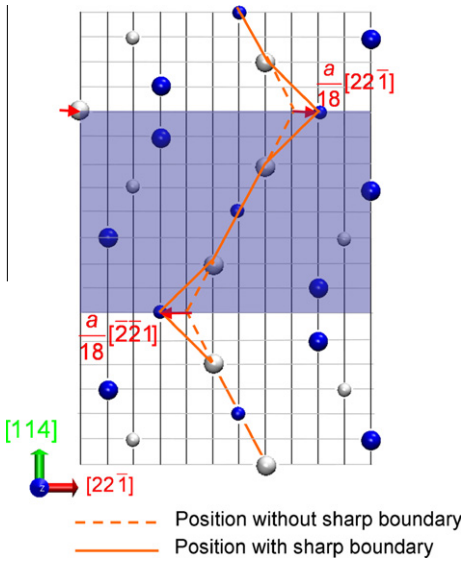

Fig. 4. Structural relaxation of an eight reflective layer twin generates a stable sharp boundary. With the sharp boundary, Ni and Ti atoms at the upper and lower boundaries have an additional shuffle of magnitude $a/18[2\ 2\ \bar{1}]$ and $a/18[\bar{2}\ \bar{2}\ 1]$, respectively.

were conducted using the density functional theory (DFT)-based Vienna Ab initio Simulation Package (VASP) [25], and the generalized gradient approximation (GGA) [26] is implemented on a projection-augmented wave (PAW). Monkhorst–Pack $9 \times 9 \times 9$ k-point meshes were used for Brillouin zone integration. The structural parameter of NiTi in B2 phase was calculated first and found to be 3.008 $\dot{A}$ with a stable energy of −6.95 eV. The procedure of shearing has been described previously [27].

To obtain the PES within reasonable computational time, we divided the shear- and shuffle-based computational domain primarily into 8×8 nodes. Additional nodes are added near the energetically significant positions such as the local minima and the saddle point. A symmetry-adapted "free energy" polynomial was fitted to our $\Delta E(\eta, \varepsilon)$ data. For this fault energy functional $F(\eta, \varepsilon) = (\Delta E(\eta, \varepsilon))$, we chose a fourth-order cosine–sine polynomial [28], which can appropriately represent the shear shuffle coupling, i.e.

$$F(\eta,\varepsilon) = \sum_{m,n=0}^{m+n\leq 4} a_{mn}[X(\eta)]^m[X(\varepsilon)]^n[1-\delta_{m0}\delta_{n0}] + \sum_{m,n=0}^{m+n\leq 4} b_{mn}[X(\eta)]^m[Y(\varepsilon)]^n \quad (1)$$

where $[X(x)] = [1 - Cos(\pi x)]$, $[Y(x)] = [Sin(\pi x)]$ and δ represents Kronecker's delta (δ_{ij} is 1(0) if i is (not) equal to j). An additional constraint of $|dF/dx|_{x=0,1} = 0$ was imposed to ensure local minima at $(0,0)$ and $(1,1)$ positions in the PES.

The transition path between local minima at the fourth layer and eighth layers was obtained from the PES with MEPs. In addition to the lowest energy path, the MEP

allowed us to identify the saddle point energy (TS), which acts as the peak barrier during the twin growth process. In this study, the MEP was calculated based on the well-established modified string method [29].

3. GPFE and GSFE in the (1 1 4) plane

The predicted energy barrier contour during the fourth to eighth layer twin formation at zero hydrostatic stress is plotted in Fig. 5a. An increase in fault energy, without any metastable position, occurs upon pure shear path ($\varepsilon = 0 \rightarrow 1$), and results in an unstable pseudo-structure with an energy maxima of 227 mJ m^{-2}. However, as we noted earlier, an additional $a/2$ shuffle of Ni and Ti in [0 0 1] and [0 0 $\bar{1}$] in the (1 1 0) plane produces a reflective twin. In PES, the stable eighth layer mirror twin is manifested with a local minima at $F(1,1)$, with an energy such that $\Delta E(\eta, \varepsilon) = 0$. We note that a mirror twinning symmetry cannot be obtained with a pure shuffle path ($\eta = 0 \rightarrow 1$). The PES plot also exhibits an extended barrier at $F(0.5, 0.5)$. At this position, the nearest-neighbor distance of Ni and Ti atoms becomes very small ($0.1667a$). The distance between atoms is an important parameter in terms of establishing the difficulty of atomic shuffling.

Three energetically significant points, local minima at the four- and eight-layer twin and the TS, are marked with dots in Fig. 5a. The position of TS at $F(0.82, 0.22)$ provides two significant conclusions: (i) the shear/shuffle mechanism is not sequential; (ii) shuffling is not a relaxation process and occurs under the application of load. In addition, the MEP provides the exact combination of the shear and shuffle magnitudes during the twin growth process. From Fig. 5a, it is clear that the path is predominantly shear at the beginning of growth (up to $\varepsilon = 0.25$). The shuffle mechanism starts at a shear of $\varepsilon = 0.25$ and nearly 1/10th of atomic shuffling ($\eta = 0.10$) has occurred, corresponding to $\varepsilon = 0.25$. A constant shear operates again up to $\varepsilon = 0.70$ and a strongly coupled shear and shuffle is effective after that until the completion of shear. The transition state is observed at this stage and the maximum peak value of 148 mJ m^{-2} corresponds to the fault energy at TS. This magnitude is very low even compared with fcc metals that

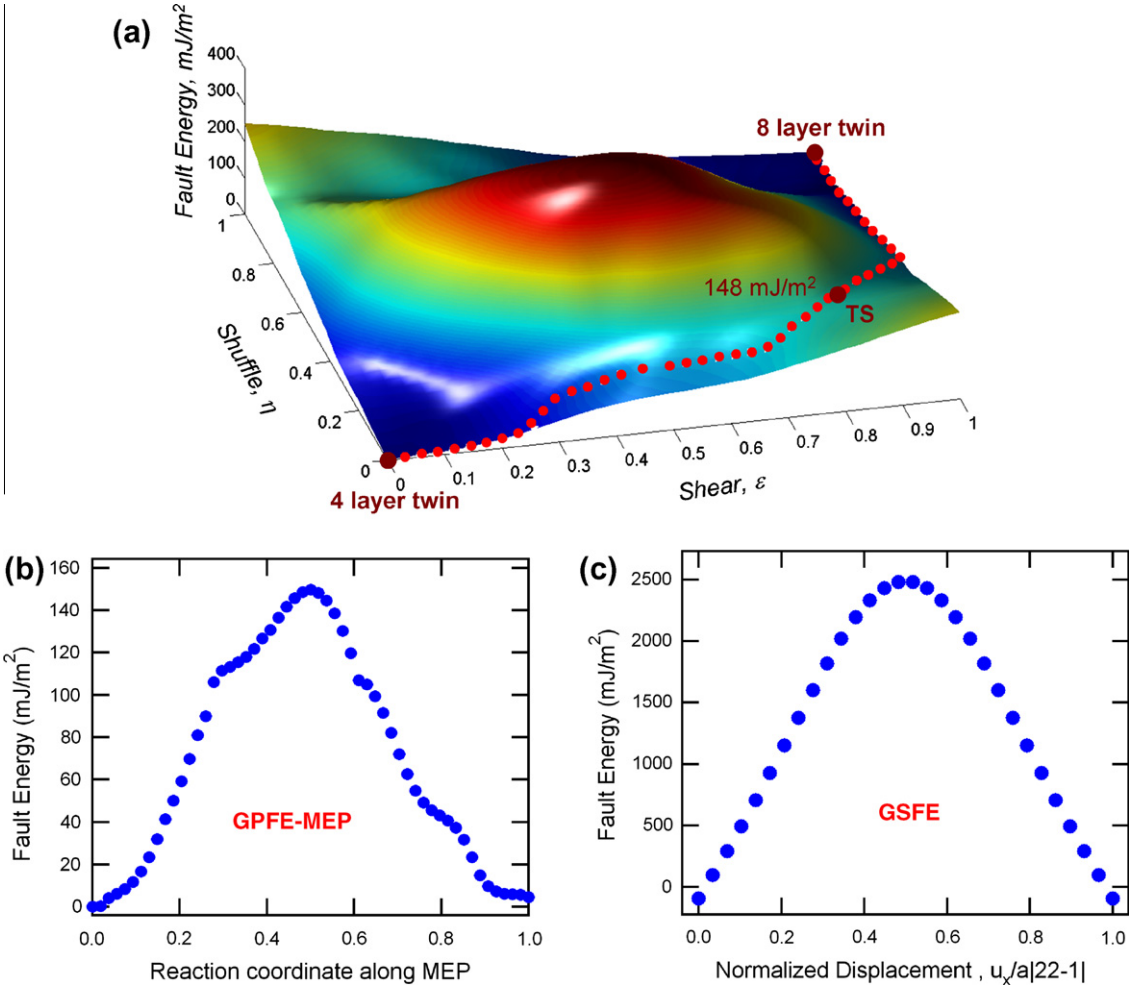

Fig. 5. (a) PES contour, MEP and TS for austenitic NiTi during twin growth in the (1 1 4)[2 2 $\bar{1}$] system. For visualization purposes, the peak point at $F(0.5, 0.5)$ has been truncated. (b) Fault energy variation is shown along the MEP. (c) GSFE curve corresponding to slip in the (1 1 4)[2 2 $\bar{1}$] system. Note that the scales in (b) and (c) are different.

undergo deformation twinning [30]. Nearly 60% of the shuffle ($0.9012\dot{A}$ out of $1.502\dot{A}$) is found to be after the complete shear and generates a B2 structure within the twin. Without the shuffle, the barrier would be much higher and will not create a perfect mirror. Also, as we noted earlier, an additional sharp boundary is added with the relaxation of atoms at the interface. This additional relaxation lowers the energy barrier at TS as compared to a completely reflective boundary at the interface. We calculated the barrier with a reflective boundary at the interface and found it to be 610 mJ m^{-2}. In comparison with 148 mJ m^{-2} this is a significantly large value. A summary of energy barriers is given in Table 3.

The fault energy during twin growth is plotted along the normalized reaction coordinate of the MEP in Fig. 5b. The fault energy curve exhibits a near-sinusoidal pattern during twin growth from four to eight layers. An asymmetry between the two sides of TS at the middle in this curve points to the complexity of coupled shear shuffle behavior. For additional twin growth (eight layers and upwards), this sinusoidal pattern is repeated with a similar coupled shear and shuffle mechanism. However, during twin nucleation (from perfect B2 to four layers of twin), the MEP might be different due to the additional elastic energy field generated from the mechanical coupling of upper and lower twin boundaries. In pure metals and alloys, the effect of mechanical coupling becomes insignificant once the twins grow more than four layers thick and the sinusoidal fault energy pattern is repeated periodically [21,30–32]. The peak energy at TS is termed the twin migration energy (γ_{TM}) since this energy is calculated relative to the stable energies of fourth or eighth layer twins.

The critical shear stress (ideal case) for twin migration can be calculated [33] as $\tau_{TMideal} = \pi\{\gamma_{TM}/\bar{b}_{twin}\}$, where $\gamma_{TM} = \gamma_{TS} - \gamma_{4/8layer}$. More sophisticated versions have been proposed incorporating the elastic energies associated with the twin nucleus [30]; this relationship, however, provides a reasonable approximation for the ideal twin migration stress. The results utilizing these formulas are provided in Table 4 for the two observed twinning modes in NiTi. In the $(1\,1\,4)[2\,2\,\bar{1}]$ and $(\bar{2}\,1\,1)[1\,1\,1]$ systems, the shear moduli are similar, and are of the order of 40 GPa using elastic constants from theory [34] and 34 GPa based on experimental findings [35]. We note that the twin growth stress in the $(1\,1\,4)$ plane is lower than in the $(\bar{2}\,1\,1)$ even though the $(\bar{2}\,1\,1)$ system has a lower energy barrier.

The proposed $(1\,1\,4)$ twin growth mechanism differs from Goo's proposal of a layer-by-layer shear with a sequential shuffle. A single-layer glide generates a pseudo-structure with an extremely high energy barrier. As noted earlier, the energy barrier for Goo et al.'s unidirectional layer-by-layer case is 1210 mJ m^{-2} as compared to the present study of 148 mJ m^{-2}, which inhibits this as a possible mechanism.

The slip barrier in a system is characterized by the GSFE curve and points out the maximum energy the atoms have to overcome during their glide in a certain plane and direction. In addition, the GSFE provides vital information about the magnitude of the Burgers vector of a possible dislocation in that particular system with a metastable position. The GSFE of the $(1\,1\,4)[2\,2\,\bar{1}]$ system was calculated by shearing one elastic halfspace of the $(1\,1\,4)$ plane relative to the other in $[2\,2\,\bar{1}]$ and is plotted in Fig. 5c. The GSFE for this system exhibits two significant features regarding possible dislocation glide: (i) the unstable fault energy is 2681 mJ m^{-2}; (ii) there is no metastable position anywhere in the system. As noted above, a metastable position indicates the possibility of dislocation splitting into twinning partials. Specifically, in order for twins to form with partials in a step-by-step process as shown in case 1 in Table 1, partials of magnitude $\bar{b} = a/18[2\,2\,\bar{1}]$ need to glide on the $(1\,1\,4)$ plane. Nevertheless, no energy well is observed once the elastic half space is sheared by a magnitude of $\bar{b} = a/18[2\,2\,\bar{1}]$. Slip nucleation can be estimated from the slope of the GSFE curve as follows, $(\tau_{SLIP})_{ideal} = \delta\gamma/\delta u_{x_{\max}}$ and the value was found to be 6.29 GPa. This stress is excessively high for glide. The absence of dislocation partial signifies that any twin formation or

Table 3
Summary of energy barriers (TS) during twin and slip.

$(1\,1\,4)[2\,2\,\bar{1}]$ Coupled shear/unidirectional shuffle (mJ m^{-2})	$(1\,1\,4)[2\,2\,\bar{1}]$ Coupled shear/bidirectional shuffle with perfect reflective boundary (mJ m^{-2})	$(1\,1\,4)[2\,2\,\bar{1}]$ Coupled shear/bidirectional shuffle with sharp boundary (mJ m^{-2})	$(1\,1\,4)[2\,2\,\bar{1}]$ Slip No reflection (mJ m^{-2})
1210	610	148	2520

Table 4
Deformation twinning elements in B2 NiTi (the shear strain is 0.707 in both cases). The critical stress for twin migration is given.

Twinning system	Twin migration energy (γ_{TM}), mJ m^{-2}	Atomic displacement ($\bar{b}$), Å	Theoretical twin migration stress ($\tau_m = \pi\gamma_{TM}/\bar{b}$) GPa	Theoretical slip stress$(\tau_{SLIP})_{ideal} = \frac{\delta\gamma}{\delta u_x}\big\vert_{\max}$ GPa
$(1\,1\,4)$ $[2\,2\,\bar{1}]$	148	2.002	2.32	6.29
$(\bar{2}\,1\,1)$ $[1\,1\,1]$	79[a]	0.867	2.86	–

[a] Ref. [21].

growth in the $(1\,1\,4)[2\,2\,\bar{1}]$ system will be in conjunction with a shear and shuffle, noted earlier as case 2.

4. Final remarks

The results point to the significance of shuffle in conjunction with shear leading to the formation of (1 1 4) twinning in NiTi. As discussed earlier, the (1 1 4) twinning vector is initially dominated by shear. However, without a shuffle, the "shear-only" mechanism generates a "pseudo-structure" with a high energy magnitude. Shuffling of atoms produces reflective twins, leading to a much lower energy position (see Table 3 for comparisons). Even though the coupling of shear and shuffle is complex, energetically the atoms have to overcome a nearly sinusoidal barrier (shown by the MEP in Fig. 5b), similar but not identical in shape to the fcc or bcc twin growth pattern [21,30]. The results are in agreement with the model formulated by Christian and Laughlin [19] and reviewed by Christian and Mahajan [20]. Our slip barrier calculation with GSFE also reveals that no twinning partial is possible for $(1\,1\,4)[2\,2\,\bar{1}]$ twinning.

We also note that our simulation results indicate a sharp boundary structure for a stable four- or eight-layer $(1\,1\,4)[2\,2\,\bar{1}]$ pattern with additional displacement at the interface. This important modification is not widely known but necessary to converge to the correct results. While translational boundary states are common for the $\sum 3$ (1 1 2) twin boundary in bcc metals [22–24], we show that similar states are also present in case of the $\sum 9$ (1 1 4) boundary in NiTi. Relaxation of the atoms near the $\sum 9$ (1 1 4) boundary in B2 NiTi allows "local" shifting at the interface. The shifting of the atoms at the boundary contributes significantly to the energy barrier of the twin growth process and, hence, needs to be accounted for.

In addition, we emphasize that the calculations undertaken consider zero hydrostatic pressure. In the presence of an elastic field of the surrounding microstructure, nonzero hydrostatic pressure effects can alter the results. This can be readily checked for a different twinning case as evidenced for (1 1 2) twins in B2 NiTi [16].

Slip deformation can occur in the B2 phase to accommodate the transformation strains or during deformation above the M_d temperature such as in an ausforming process. In the studies of Chumlyakov and co-workers [8,9], and Tyumentsev et al. [36], the NiTi is deformed at higher temperatures where both slip and twinning occurs. The slip systems were identified as $\langle 0\,1\,0\rangle\{1\,1\,0\}$ and $\langle 0\,1\,0\rangle\{1\,0\,0\}$ consistent with Moberly et al.'s results [6]. More recently Simon et al. [37] and Norfleet et al. [3] have provided precise details of transformation-induced plasticity, confirming early findings [8]. The selection of slip or twinning as a deformation mechanism depends on the stress state in the crystal. Loading orientations near [0 0 1] in compression have been observed to preclude slip deformation and result in twinning.

Deformation by slip is assisted by dislocation glide and is rather simple to comprehend. As discussed earlier, the twinning mechanism in B2 is much more complicated than pure shear deformation. A better understanding of the plastic flow behavior of the B2 structure is essential. Our calculations show that for the case of B2 twinning, the twinning stresses are of the order of 2–3 GPa. Our previous experiments in compression show stresses exceeding 2 GPa [38] in general agreement with theory.

Several other techniques, such as molecular dynamics or molecular statics with a twinning defect can be utilized to calculate the energy barriers during twin migration. However, these methods rely on semi-empirical interatomic potentials, and reliable potentials for B2 NiTi are only at an early stage of development. Hence, a DFT-based first-principles electronic structure calculation was utilized to calculate the planar fault energy barriers. Admittedly, the GPFE method of interfaces needs to be augmented with dislocation theory for evaluation of the entire energy, which would lead to determination of the stress required for twin migration in the presence of defects. Such a calculation, via energy minimization, has been demonstrated for simple metals in our early work [30] but such a complete calculation is not possible for NiTi yet in view of the complexity of the twin formation. However, this type of approach does not affect the overall outcome, i.e. the mechanism suggested.

The paper highlights the profound contribution of shuffle on the energy surfaces, the growth of four layers constituting a twin, and the complexities associated with sharp boundary effects at twin–matrix interfaces. At this time, the complete energy description is not amenable to formulations utilizing the Peierls barrier approach in conjunction with GSFE as emphasized in our early work [39]. Such a "perfect" approach is not possible at this time because the description of shuffles, as distinct from shears, in the framework of an energy description has not been satisfactorily resolved. The approach we have undertaken utilizing DFT has the usual approximations inherent with this methodology regarding the finite box size (which has been optimized to assure convergence), the lack of thermal activation, and study of static configurations as noted previously.

In summary, we have made advances towards a quantitative understanding of the deformation twinning in NiTi austenite. The (1 1 4) twin growth mechanism in B2 NiTi has been addressed utilizing first-principles calculations. The energy landscape reveals a clear coupling of shear and shuffle mechanism with barriers of the order of 150 mJ m^{-2}. The results explain why $(1\,1\,4)[2\,2\,\bar{1}]$ twin systems have been observed experimentally. The closest competitor to (1 1 4) twinning is (1 1 2) twinning, and we show why it is not surprising to see both in view of their similar twin stress magnitudes. Overall, we provide an improved understanding of shape memory alloys by categorization of their twinning behavior (particularly for two cases,

where the first is aided by partial dislocations and the second does not involve partial dislocations).

Acknowledgements

The work is supported by the National Science Foundation under DMR-0803270. We acknowledge earlier discussions with Prof. D.D. Johnson on PES. The authors gratefully acknowledge the use of the parallel computing resources part of the Taub cluster provided by the Computational Science and Engineering Program at the University of Illinois, and also partial support from CMMI-1130031.

References

[1] Otsuka K, Wayman CM, editors. Shape memory materials. Cambridge: Cambridge University Press; 1998.
[2] Duerig TW. Mater Sci Eng A 2006;438-440:69.
[3] Norfleet DM, Sarosi PM, Manchiraju S, Wagner MFX, Uchic MD, Anderson PM, et al. Acta Mater 2009;57:3549.
[4] Moberly WJ. Mechanical twinning and twinless martensite in ternary Ti50Ni(50-x)Mx intermetallics. PhD thesis, Stanford University; 1991.
[5] Moberly WJ, Proft JL, Duerig TW, Pelton AR, Sinclair R. Thermomechanical strengthening of B2 intermetallics. New Orleans, LA: Minerals, Metals & Materials Soc. (TMS); 1991. p. 387.
[6] Moberly WJ, Proft JL, Duerig TW, Sinclair R. Acta Metall Mater 1990;38:2601.
[7] Goo E, Duerig T, Melton K, Sinclair R. Acta Metall 1985;33:1725.
[8] Surikova NS, Chumlyakov YI. Phys Metals Metallogr 2000;89:196.
[9] Chumlyakov Y, Kireeva I, Panchenko E, Timofeeva E, Pobedennaya Z, Chusov S, et al. Russ Phys J 2008;51:1016.
[10] Ii S, Yamauchi K, Maruhashi Y, Nishida M. Scripta Mater 2003;49:723.
[11] Nishida M, Matsuda M, Fujimoto T, Tanka K, Kakisaka A, Nakashima H. Mater Sci Eng A 2006;438-440:495.
[12] Ezaz T, Sangid MD, Sehitoglu H. Philos Mag 2011;91:1464.
[13] Bilby BA, Crocker AG. Proc R Soc Lond, Series A 1965;288:240.
[14] Cahn RW. Adv Phys 1954;3:363.
[15] Krishnan M, Maji BC. Philos Mag Lett 2001;81:243.
[16] Ezaz T, Sehitoglu H. Appl Phys Lett 2011;98:241906.
[17] Chu F, Pope DP. Mater Sci Eng A 1993;A170:39.
[18] Yoo MH, Fu CL, Lee JK. Journal de Phsique 1991;1:1065.
[19] Christian JW, Laughlin DE. Acta Metall 1988;36:1617.
[20] Christian JW, Mahajan S. Prog Mater Sci 1995;39:1.
[21] Ogata S, Ju L, Yip S. Phys Rev B 2005;71:224102.
[22] Beauchamp P. Philos Mag A 1978;37:167.
[23] Bevis M, Vitek V. Scripta Metall 1970;4:719.
[24] Mrovec M, Ochs T, Elsasser C, Vitek V, Nguyen-Manh D, Pettifor DG. Z Metall 2003;94:244.
[25] Kresse G, Hafner J. Phys Rev B 1993;48:13115.
[26] Perdew JP, Burke K, Ernzerhof M. Phys Rev Lett 1996;77:3865.
[27] Ezaz T, Sehitoglu H. Appl Phys Lett 2011;98:141906.
[28] Liu JB, Johnson DD. Phys Rev B 2009;79:134113.
[29] Maragliano L, Fischer A, Vanden-Eijnden E, Ciccotti G. J Chem Phys 2006;125:24106.
[30] Kibey S, Liu JB, Johnson DD, Sehitoglu H. Acta Mater 2007;55:6843.
[31] Ezaz T, Sehitoglu H. Appl Phys Lett 2011;98:141906.
[32] Ezaz T, Sehitoglu H. Acta Mater; 2011. doi:10.1016/j.actamat.2011.05.063.
[33] Venables JA. Philos Mag 1961;6:379.
[34] Hatcher N, Kontsevoi OY, Freeman AJ. Phys Rev B 2009;80:144203. 18 pp.
[35] Brill TM, Mittelbach S, Assmus W, Mullner M, Luthi B. J Phys: Condensed Matter 1991;3:9621.
[36] Tyumentsev AN, Surikova NS, Litovchenko IY, Pinzhin YP, Korotaev AD, Lysenko OV. Acta Mater 2004;52:2067.
[37] Simon T, Kroger A, Somsen C, Dlouhy A, Eggeler G. Acta Mater 2010;58:1850.
[38] Sehitoglu H, Jun J, Zhang X, Karaman I, Chumlyakov Y, Maier HJ, et al. Acta Mater 2001;49:3609.
[39] Kibey S, Liu JB, Curtis MJ, Johnson DD, Sehitoglu H. Acta Mater 2006;54:2991.